GEOPHYSICAL RESEARCH LETTERS, VOL. 27, NO. 22, PAGES 3651-3654, NOVEMBER 15, 2000

Co-seismic deformation during the M_w 7.3 Aqaba earthquake (1995) from ERS-SAR interferometry

Yann Klinger,[1] Rémi Michel, Jean-Philippe Avouac

Laboratoire de Détection et de Géophysique, Commisariat à l'Energie Atomique, Bruyères-le-Châtel, France

Abstract. The M_w 7.3 1995 Aqaba earthquake is the largest instrumental earthquake along the Dead Sea Fault. We complement previous seismological studies by analyzing co-seismic ground displacement from differential interferometry computed from ERS images spanning 3 different areas. They are compared with a synthetic model derived from seismological study. Only far-field deformation related to the main sub-event could be revealed because the near-field area lies within the gulf. The interferometric data imply a 56 km long and 10 km wide fault segment, connecting the Elat Deep to the Aragonese Deep, which strikes N195°E and dips 65°to the west, with 2.1 m left-lateral slip and a 15.5°rake indicating a slight normal component. The geodetic moment compares well with the seismic moment.

1. Introduction

On November 22, 1995 a M_w 7.3 earthquake occurred in the Gulf of Aqaba, at the southern end of the Dead Sea fault (DSF). This event is the largest instrumental earthquake along the DSF and is comparable to the largest historical earthquakes documented along the DSF [*e.g., Ambraseys et al.,* 1994]. In the present case, little is known about the exact fault location and geometry because the epicenter was located offshore, about 60 km south of the tip of the gulf (Figure 1). Ground ruptures were reported at various places around the northern part of the gulf that reflect more probably superficial gravity-induced tectonics along the steep flanks of the gulf rather than primary ruptures [*El-Hakim,* 1996; *Wurst et al.,* 1997; *Baer et al.,* 1999; *Klinger et al.,* 1999]. This study complements previous seismological investigations [*Fattah et al.,* 1997; *Pinar and Türkelli,* 1997; *Klinger et al.,* 1999] by analyzing co-seismic ground displacements determined from 3 differential interferograms computed from ERS SAR images (Figure 1 and Table 1).

2. Active Tectonic Background

The 1200 km long DSF is a major left-lateral strike-slip fault, separating the Africa plate from the Arabia plate (inset in Figure 1). The Gulf of Aqaba is formed of three pull-apart basins, the Elat Deep, the Aragonese Deep and the Daka Deep from north to south. They are connected by *en echelon* strike-slip faults striking about N20°[*Ben-Avraham,* 1985] (Figure 1). The gulf is only 25 km wide but it reaches a depth of more than −1800 m and the surrounding Sinai and Hedjaz mountain ranges peak to more than 2600 m. The tectonic significance of these large topography is still unclear since it might be related either to Neogene rifting or present tectonics [*Ben-Avraham and Zoback,* 1992].

2.1. Background Seismicity in the Gulf of Aqaba

Two large earthquakes of magnitudes ~7 are known from historical records to have occurred near the northern tip of the Gulf of Aqaba, in 1068 and 1212 [*Abou Karaki,* 1987; *Ambraseys et al.,* 1994; *Zilberman et al.,* 1998]. Since the beginning of instrumental monitoring, the Gulf of Aqaba is one of the most seismically active zone along the DSF. In addition to the M_w 7.3 earthquake of 1995, three seismic swarms were recorded in

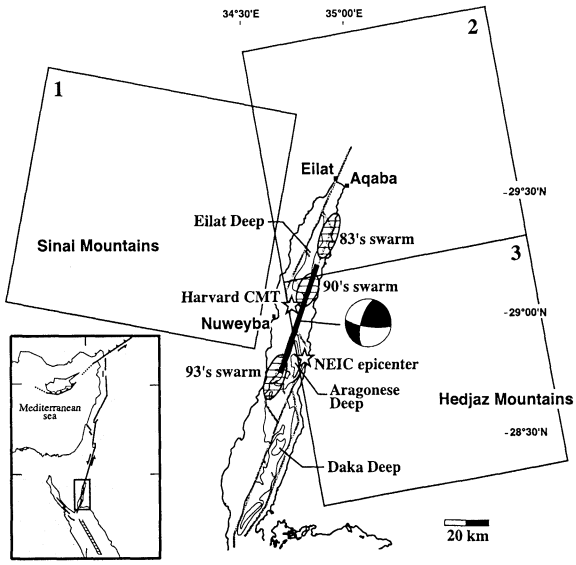

Figure 1. Seismotectonic map of the Gulf of Aqaba adapted from *Ben Avraham* [1985]. Dashed areas show extent of 1983, 1990 and 1993 seismic swarms. Stars represent epicenter and centroid. The trace at the bottom of the gulf of the best fault segment modeled in this study (black segment), and associated focal mechanism (see Table 2) are indicated. Black boxes depict location of interferograms.

[1]Now at SeismoLab., California Institute of Technology, Pasadena, California

Paper number 1999GL008463.
0094-8276/00/1999GL008463$05.00

Table 1. Single Look Complex SAR images used to compute interferograms of Figure 2a and 3. See Figure 1 for location of the 3 zones.

Zone	Satellite	Date	Orbit	Frame
1	ERS2	06/09/95	705	3015
	ERS2	05/24/96	5715	3015
2	ERS1	03/29/95	19369	585
	ERS1	11/29/95	22876	585
3	ERS1	08/16/95	21373	567
	ERS2	08/21/97	12221	567

1983, 1990 and 1993 which affected different parts of the gulf, with magnitudes up to ~6 [*El-Isa et al.*, 1984; *Abou Karaki et al.*, 1993] (Figure 1). These swarms probably relate to episodes of extensional faulting on ~NS trending normal faults as indicated by the focal mechanism of the largest shock in 1993 [*e.g. Fattah et al.*, 1997].

2.2. The Earthquake of M_w 7.3, November 22, 1995

Several seismological studies have already addressed the rupture process of the 1995 earthquake [*Fattah et al.*, 1997; *Pinar and Türkelli*, 1997; *Klinger et al.*, 1999; *Baer et al.*, 1999]. They all point to a complex seismic source with 2 or 3 sub-events on distinct fault segments. According to the inversion of broad-band body-waves and aftershock relocation [*Klinger et al.*, 1999], the largest sub-event would have released about 70% of the total seismic moment as left-lateral slip on a N200°E striking fault, dipping about 74°to the west. The 5°seismologically determined rake indicates only a slight dip-slip component. The two other sub-events occurred on sub-parallel fault segments with a larger vertical component. Although the relative position of the three fault segments and the timing of the rupture is reasonably well documented, the exact location and geometry of the main fault segment could not be tightly constrained [*Klinger et al.*, 1999]. The accurate determination of the location and geometry of the main sub-event from seismology is indeed a non-trivial question due to the spatial extent of the seismic source, as illustrated by the difference between the positions of the epicenter and centroid, respectively (Figure 1, stars).

3. Co-Seismic Deformations from Differential SAR Interferometry

Differential SAR interferometry can measure coseismic surface displacements at the millimeter scale from the phase difference between two radar images collected on successive tracks over the same area [*e.g. Pelzer and Rozen*, 1995]. Using C-band radar imagery, interferometry provides the satellite-to-ground component of the ground displacement, modulo 2.8 cm, that occurred in the time span between the two acquisitions [*e.g. Massonnet and Feigl*, 1998]. The technique is particularly well adapted to desert areas where decorrelation factors are not too limiting, like the region of Aqaba.

3.1. Data Processing

We used ERS-1 and ERS-2 Single Look Complex data covering 3 frames (Table 1) around the northern tip of the gulf (Figure 1). A key parameter in the computation of an interferogram is the baseline (i.e. the distance between the orbital positions) which is generally known with an accuracy of several meters. An eventual artifact, caused by this uncertainty, consists of a nearly constant gradient of deformation, not related to any ground displacement, that may account for about 6 cm ground relative displacement distributed across the image. We have therefore slightly adjusted the baselines in order to minimize the interferometric signal away from the fault zone where large gradients of ground displacement are unexpected.

The ERS images were processed following the procedure described in *Michel et al.* [1999]. We used the 30 arc-second DCW Digital Elevation Model to remove

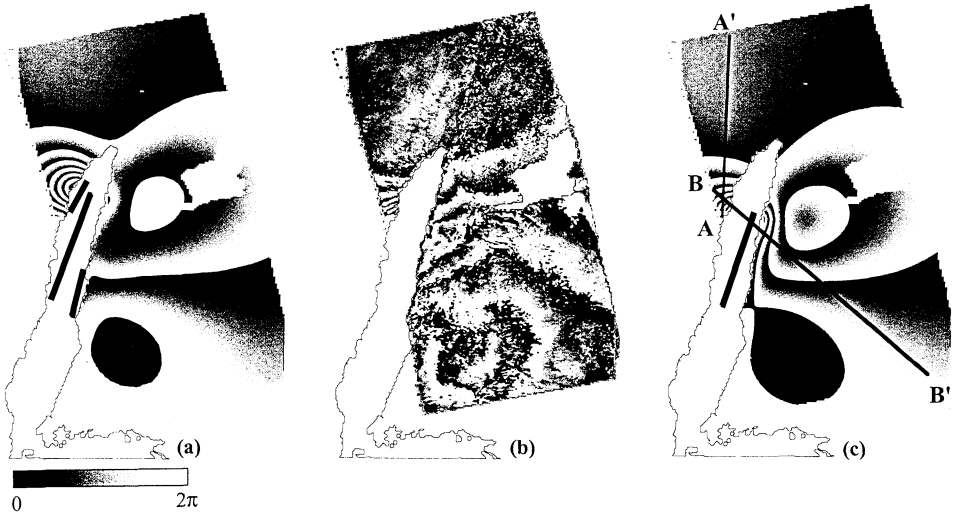

Figure 2. a) Synthetic interferogram computed from seismological modeling after *Klinger et al.*, [1999]. b) Differential SAR interferogram over zones 2 and 3 (see Table 1). Average noise is 5 mm (rms). Projection vector (-0.38; -0.061; 0.92). c) Best modeled synthetic interferogram. Black lines show location of faults. Fringe patterns in Figures 2a and 2b are fairly consistent. Some discrepancies remain, however, along the western coast.

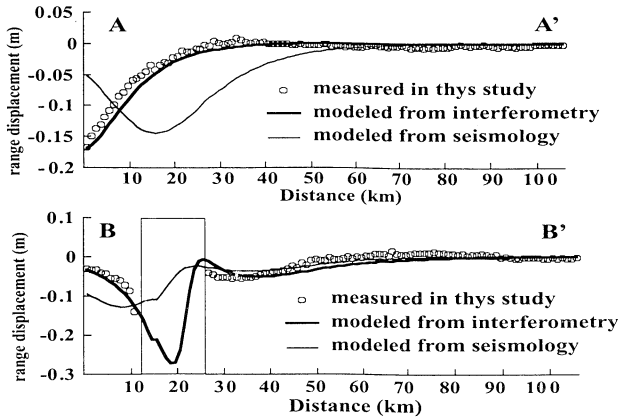

Figure 3. Comparison between ground displacements along the radar line of sight. 1) measured from unwrapped interferogram, 2) computed from the seismological model [*Klinger et al.* 1999] and 3) modeled in this study . See Figure 2c for location of profiles. Gray box denotes location of the gulf.

topographic fringes. The baselines used in this study are smaller than 30 m leading to a residual topographic noise (resulting from errors in the DEM) of less than 5 mm on the measured ground displacement. Images from other frames were also available but were discarded because their baseline were too large compared to the quality of the DEM. The uncertainties on the measured ground displacements may then be modeled as a white noise with an amplitude of about 5 mm rms and a low frequency noise with an amplitude of about 6 cm that may result from atmospheric noise or uncertainties in the estimates of orbital parameters. The interferogram covering zone 1, west of the gulf, does not show any significant geodetic signal as expected from the theoretical model. By contrast, the interferograms computed from the eastern frames in zones 2 and 3 show fringes that are clearly related to ground displacement (Figure 2b) and that differ from the ones computed from the initial three sub-event sources model proposed by *Klinger et al.* [1999] (Figure 2a) using *Okada*'s [1985] analytical formulation.

3.2. Analysis of the Interferograms

We have modified the fault model proposed by *Klinger et al.* [1999], in order to better fit the measured differential interferograms. Tests have shown that the signal due to the two small sub-events is overwhelmed by the co-seismic deformation induced by the main sub-event, which accounts for all of of the fringes that are shown

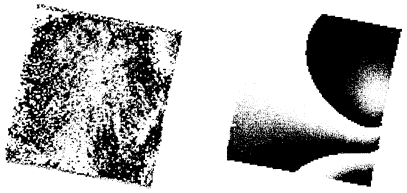

Figure 4. Measured and best fitted interferograms over zone 1. Projection vector (0.38; -0.08; 0.92). Average deformations are consistent but further interpretation is not reasonable due to low amplitude of observed and modeled deformation compared to the noise in the interferogram.

in Figure 2a. So, because no data are available on the near-field area that lies under water, only the location and geometry of the main sub-event might be retrieved from our interferograms.

The measured and seismologically predicted interferograms (Figure 2a,b) show similarities, but the synthetic fringes extend too far to the north. On the eastern coast, the amplitude of the synthetic deformation is lower than the measured one, suggesting that the main segment probably lies farther away from the coast. These offsets are compared on profiles across the unwrapped measured and synthetic interferograms (Figure 3).

Later we adjusted the parameters of the seismic source model by trial and error. We considered only one planar dislocation to get the results shown in Figure 2c and Table 2. A fault slightly shorter and shifted to the south and east from to the position of the main sub-event of the initial model provided the best fitting model. The 1.9 cm rms residual error between the modeled and observed ground displacement fields is comparable to the noise level in the measurements so that the data do not require any more sophisticated modeling (Figure 3). The fringe pattern in Figure 2c is indeed similar to the measurements in Figure 2b. The high gradient of deformation, indicating a depression towards the gulf along the western coast, is well modelled. On the eastern side, the circular fringe pattern is also reasonably well fitted. Some discrepancies remain that might be partly due to the use of *Okada*'s [1985] analytical formulation, which assumes only an elastic half-space with a horizontal free surface and does not account for the large topographic variations of the area. In zone 1 the adjusted model predicts a low signal consistent with the absence of any clear residual fringes obtained in the interferogram (Figure 4).

Table 2. Best model adapted from the seismological model of *Klinger et al.*, [1999] to fit the unwrapped interferograms of Figure 2a. Angles are given in degrees, azimuth is given clockwise from North. fault reach the bottom of the Gulf.

	Latitude	Longitude	Length (km)	Azimuth	Dip	Depth (km)	Rake	Slip (m)
Klinger et al.,	28.829	34.825	27.4	191.6	58.6	14	−21.2	0.42
[1999]	29.042	34.777	61.0	199.3	74.3	14	−5.0	2.5
	29.277	34.786	25.6	24.7	67.2	1.1	−8.5	0.74
This study	28.93	34.78	56	195.15	65	12	−15.5	2.1

The proposed model thus appears to provide an acceptable fit to the observed interferograms and is characterized by a fault geometry relatively close to that derived from seismological investigations (Table 2). The M_w 7.1 moment magnitude computed from this model (following *Aki and Richards* [1981], $\mu = 3.3\ 10^{10}$ N/m) compares well with the value of M_w 7.2 assigned to the main sub-event from body-waves analysis [*Pinar et Türkelli,* 1997; *Klinger et al.,* 1999].

4. Conclusions and Implications

This study brings new constraints to the location and geometry of the main sub-event of the 1995 Aqaba earthquake. It implies a dominantly strike-slip fault dipping about 65°to the west with a slight normal component, connecting the Aragonese Deep to the Elat Deep. Thus the pull-apart basins seems to be only activated by small earthquakes, with magnitude $M_w \lesssim 6$ and a significant dip-slip component, that occur either in swarms or in association with larger events on the connecting strike-slip faults. The strike-slip segments in the Gulf of Aqaba are also associated with a minor dip-slip component that can also, when accumulated over time, contribute to the building of the gulf morphology. It is particularly striking that the local zone of subsidence at the southern end of the Elat Deep closely mimics the gulf morphology in that area (see profiles AA′and BB′in Figure 3). The morphology of the Gulf of Aqaba most probably reflects present tectonics and would have resulted from the accumulation of co-seismic deformation alike that produced by the 1995 earthquake, together with normal faulting within the pull-apart basins.

Acknowledgments. This study was completed partially at Institut de Physique du Globe de Strasbourg URM 7516, France. ERS SAR images were provided by ESA under AO3.253. We thank two anonymous reviewers for their helpful reviews.

References

Abou Karaki N., Synthèse et carte sismotectonique des pays de la bordure orientale de la Méditerranée : sismicité du système de failles du Jourdain-Mer Morte, Ph.D. thesis, Strasbourg I Univ. (France), 1987.

Abou Karaki N., L. Dorbath, H. Haessler, La crise sismique du golfe d'Aqaba de 1983 : implication tectonique, *C. R. Acad. Sci. Paris, 317,* 1411-1416, 1993.

Aki K., P.G. Richards, *Quantitative seismology,* Freeman and Comp., San Francisco, 1981.

Ambraseys N.N., C.P. Melville, R.D. Adams, *The seismicity of Egypt, Arabia and the Red Sea, an historical review,* Cambridge Univ. Press, 1994.

Baer G., D. Sandwell, S. Williams, Y. Bock, G. Shamir, Coseismic deformations associated with the November 1995, M_w=7.1 Nuweiba earthquake, Gulf of Elat (Aqaba), detected by synthetic aperture radar interferometry, *J. Geophys. Res., 104,* 25221-25232, 1999.

Ben-Avraham Z., Structural framework of the gulf of Elat (Aqaba), northern Red Sea, *J. Geophys. Res., 90,* 703-726, 1985.

Ben-Avraham Z., M.D. Zoback, Transform-normal extension and asymmetric basins: an alternative to pull-apart models, *Geology, 20,* 423-426, 1992.

Dziewonski A.M., G. Ekstrom, M.P. Salganik, Centroid-Moment tensor solution for October-December 1995, *Phys. Earth Planet. Inter., 101,* 1-12, 1997.

El-Hakim B.A., The Aqaba 95 earthquake A quick review, *Egyptian Geological Survey and Mining Authority Report,* Cairo, Egypt, 1996.

El-Isa Z.H., H.M. Merghelani, M.A. Bazzari, The gulf of Aqaba earthquake swarm of 1983 January-April, *Geophys. J. R. Astron. Soc., 86,* 413-424, 1984.

Fattah A.K.A., H.M. Hussein, E.M. Ibrahim, A.S. Abu El Atta, Fault plane solutions of the 1993 and 1995 gulf of Aqaba earthquakes and their tectonic implications, *Annali di Geofisica, 40,* 1555-1564, 1997.

Klinger Y., L. Rivera, H. Haessler, J.C. Maurin, Active faulting in the gulf of Aqaba : new knowledge from the Mw 7.3 earthquake of November 22, 1995, *Bull. Seismol. Soc. Am., 89,* 1025-1036, 1999.

Massonnet, D. and K.L. Feigl, Application of ERS-1 radar interferometry to the Landers Earthquake, *Rev. Geophys., 36,* 4, 441-500, 1998.

Michel, R., J.P. Avouac and J. Taboury, Measuring near field ground displacements from SAR images : application to the Landers earthquake, *Geophys. Res. Lett., 26,* 3017-3020, 1999.

Okada Y., Surface deformation due to shear and tensile faults in an half-space, *Bull. Seismol. Soc. Am., 75,* 1135-1154, 1985.

Peltzer G., P. Rosen, Surface displacement of the 17 May 1993 Eureka Valley, California, earthquake observed by SAR interferometry, *Science, 268,* 1333-1336, 1995.

Pinar A., N. Türkelli, Source inversion of the 1993 and 1995 gulf of Aqaba earthquake, *Tectonophysics, 283,* 279-288, 1997.

Wurst H. and many others, Post-seismic analysis of failure features and seismic hazard implication, *Geological Survey of Israël Report GSI/3/97,* Israël, 1997.

Zebker, H.A. and J. Villasenor, Decorrelation in interferometric radar echoes, *IEEE Trans. Geo. Rem. Sens., 30,* 5, 950-959, 1992.

Zilberman E., R. Amit, N. Porat, U. Avner, Relocalisation of the epicenter of the 1068 earthquake in the Avrona playa, southern Dead Sea rift, using paleoseismic and archeoseismic evidences.paper presented at ESC 26th (Abstract), Tel-Aviv, Israël, 1998.

Y. Klinger, SeismoLab #100-23, California Institute of Technology, Pasadena, CA 91125, USA, (e-mail: yann@gps.caltech.edu)

J. P. Avouac and R. Michel, LDG, CEA, BP12, 91680 Bruyères-le-Châtel,France,(e-mail: michel@dase.bruyeres.cea.fr, avouac@dase.bruyeres.cea.fr)

(Received December 12, 1999; revised April 25, 2000; accepted September 15, 2000.)